Biomicrofluidics

# Magnetic nanotechnology for circulating tumor biomarkers screening: Rational design, microfluidics integration and applications

Cite as: Biomicrofluidics **13**, 051501 (2019); https://doi.org/10.1063/1.5119052
Submitted: 08 July 2019 . Accepted: 27 August 2019 . Published Online: 10 September 2019

Nanjing Hao, and John X. J. Zhang

**COLLECTIONS**

Paper published as part of the special topic on Microfluidics, Circulating Biomarkers and Cancer
Note: This paper is part of the special issue on Microfluidics, Circulating Biomarkers and Cancer.

Biomicrofluidics REVIEW scitation.org/journal/bmf

# Magnetic nanotechnology for circulating tumor biomarkers screening: Rational design, microfluidics integration and applications

Cite as: Biomicrofluidics 13, 051501 (2019); doi: 10.1063/1.5119052
Submitted: 8 July 2019 · Accepted: 27 August 2019 ·
Published Online: 10 September 2019



Nanjing Hao and John X. J. Zhang[a)]

## AFFILIATIONS

Thayer School of Engineering, Dartmouth College, 14 Engineering Drive, Hanover, New Hampshire 03755, USA

**Note:** This paper is part of the special issue on Microfluidics, Circulating Biomarkers and Cancer.
[a)]**E-mail:** john.zhang@dartmouth.edu

## ABSTRACT

Magnetic nanotechnology represents a major and promising frontier with great potential to significantly advance the field of liquid biopsies. The last decade has witnessed considerable progress in the research and development of magnetic nanosystems for circulating tumor biomarkers screening. With the emergence of microfluidics, both rational design of magnetic nanomaterials from microfluidic reactors and efficient magnetic screening of circulating tumor biomarkers from microfluidic chips become available. This review focuses on recent advances of magnetic nanoparticles for the screening of circulating tumor biomarkers including circulating tumor cells, exosomes, and nucleic acids. We summarize the established conventional magnetic nanosystems for circulating tumor biomarkers screening, highlight microfluidic reactors-enabled magnetic nanoparticles synthesis, and discuss the emerging roles of microfluidic chips in magnetic screening of circulating tumor biomarkers. In addition, the current challenges and opportunities are provided for guiding future studies.



## I. INTRODUCTION

Liquid biopsies hold great promises to enable what conventional tissue biopsies could not such as early detection, real-time monitoring, and noninvasive sampling of biological fluids to guide point-of-care treatment. Particularly, circulating tumor cells (CTCs), exosomes, and nucleic acids representing three typical circulating tumor biomarkers of liquid biopsies have received great attention since they can provide key insights into tumor burden, intratumoral heterogeneity, and therapy response.[1,2] In recent years, significant technique advances have been achieved toward screening, identification, and characterization of tumor biomarkers.[2] Among these techniques, magnetic assays (especially antibody-conjugated immunomagnetic nanoassays) have attracted considerable interest from researchers due to ease of operation, simple collection, facile particle surface functionalization, good specificity, and high throughput.[3,4] Actually, since the CellSearch™ immunomagnetic assay was approved by the U.S. Food and Drug Administration in January 2004 for the detection of circulating breast cancer cells, a large number of studies have been devoted to magnetic screening of circulating tumor biomarkers.

The emergence of microfluidics provides new and unique opportunities for chemical and biomedical engineering.[5–9] By virtue of low sample consumption, high flexibility, enhanced spatiotemporal control, and automated precise operation, microfluidics has a great potential for the rational design of magnetic nanomaterials toward liquid biopsies. Specifically, from materials synthesis aspect, microfluidics-based reactors (microreactors) offer many superior features that conventional batch reactors can hardly achieve. These include but are not limited to (1) rapid reaction kinetics for fast screening of material properties; (2) intensive mixing of reactants inside the microchannel for achieving high yields; (3) greatly reduced reactor dimensions and automated operations for allowing reproducible synthesis of high quality products; and (4) confining active starting reactants into a small space for offering great chances to create new materials.[10–14] Parallelly, from the liquid biopsy aspect, microfluidics-based chips (microchips) also exhibit great features over conventional screening approaches, such as minute volume of sample consumption, short analysis time, high sensitivity, good system integration, and precise process control.[15] These advantages enable microfluidics to serve as an

emerging and promising platform for effective and efficient screening of circulating tumor biomarkers.

The scope of this review is intended to present an overview of recent progress on the magnetic screening of circulating tumor biomarkers including circulating tumor cells, exosomes, and nucleic acids. We start to discuss the established conventional magnetic approaches for circulating tumor biomarkers screening, followed by highlighting the important roles of microfluidic reactors in the rational design of magnetic nanomaterials, and then summarize the applications of microfluidic chips in magnetic screening of circulating tumor biomarkers. Finally, we point out the current challenges and opportunities for guiding future studies in this area.

## II. CONVENTIONAL APPROACHES FOR MAGNETIC SCREENING OF CIRCULATING TUMOR BIOMARKERS

### A. Magnetic materials synthesis from batch reactors

For magnetic screening of circulating tumor biomarkers, magnetic materials need to be utilized to interact with target biomarkers and then separate them by an applied external magnetic field. To date, numerous synthesis methods have been developed to synthesize magnetic nanoparticles from conventional flask-based batch reactors. These methods, including coprecipitation, thermal decomposition, hydrothermal reaction, solgel, microemulsion, biosynthesis, sonolysis, electrochemical reaction, microwave-assisted synthesis, and laser pyrolysis, have already been systematically discussed in many previous literature,[16–22] which are beyond the scope of this review. Through batch reactors, magnetic materials with different sizes (from a few nanometers to hundreds of micrometers), shapes (such as sphere, rod, ellipsoid, cube, and wire), and compositions (such as Fe, Co, Ni, $Fe_3O_4$, $Fe_2O_3$, and magnetic hybrids) are already available.

### B. Magnetic screening of circulating tumor biomarkers from bulk techniques

Compared to well-established batch synthesis systems, applications of magnetic particles for circulating tumor biomarkers screening are largely lagging behind because of lack of understanding across disciplines. As shown in Table I, current magnetic materials for tumor biomarkers screening are mainly antibody-conjugated spherical iron oxides ($Fe_3O_4$ or $Fe_2O_3$). Specifically, from a materials design viewpoint, (1) magnetic particle types are always iron oxides ($Fe_3O_4$ or $Fe_2O_3$) and of which many of them are micrometer-sized beads. Although magnetic beads are commercially available from several manufacturers such as Invitrogen, R&D Systems, Miltenyi Biotec, Chemicell, and Ocean NanoTech, the particle size is generally large and only spheres are displaying. In addition, there is still no sufficient direct evidence to show a correlation between particle size and tumor biomarkers screening. (2) Almost all these studies utilize spherical-shaped magnetic particles. Although nonspherical particles exhibit superior biological performance over their spherical counterparts,[23–32] very few studies paid attention to the roles of particle shape in tumor biomarkers capture. (3) Single and simple surface functionalization. Although antibodies (such as anti-EpCAM or anti-HER2) are employed to recognize specific biomarkers, the conjugation density, stability, and target efficiency of antibodies are easily neglected. It is also noted that, considering the heterogeneity of circulating tumor biomarkers, using multiple antibodies as a "cocktail" should be ideal strategies. However, the design and optimization approaches are still rarely reported.

To date, a large number of studies have demonstrated the feasibility of bulk magnetic techniques in the screening of circulating tumor cells, exosomes, and nucleic acids (Table I), even though a majority of them focused on the cell level performance. However, the effect of the physicochemical properties of magnetic materials (such as size, shape, and surface chemistry) on the capture efficiency of tumor biomarkers has yet rarely been investigated.

Particle size has long been known for dominating the interactions of cells with nanoparticles.[69–72] In general, smaller-sized particles show faster reaction kinetics with cells, which may result in higher capture efficiency of tumor cells. The size effect of magnetic particles in the screening of CTCs was first revealed in one recent study where researchers compared the capture efficiency of 25 nm, 150 nm, and 1 $\mu$m sized magnetic beads [Fig. 1(a)].[63] The results showed that the smaller the particle size, the higher the capture efficiency of tumor cells. Specifically, 25 nm magnetic particles have the highest capture efficiency (82.2%), followed by 150 nm particles (77.7%), and 1 $\mu$m particles have the relatively lowest level (60.4%). In addition, 25 nm particles could capture model CTCs over 80% efficiency even at concentrations as low as ~25 cells/ml. Therefore, rational design of particle size may greatly help to maximize the screening efficiency and detection sensitivity of CTCs.

Similar to particle size, particle shape also plays an important role in the biological performance of micro-/nanomaterials. In recent years, more and more evidence demonstrated that nonspherical particles exhibit enhanced cellular activities over their spherical counterparts.[24,73–75] However, little attention was paid to liquid biopsies. Actually, the effect of particle shape in the screening of CTCs was still unclear until one recent study revealed it. Compared to sphere-shaped magnetic mesoporous silica nanoparticles, rod-shaped ones were found to exhibit faster magnetic isolation as well as better performance in the screening of CTCs in spiked cells [Fig. 1(b)].[55] Importantly, in real clinical blood samples, the CTCs capture rate of rod-shaped particles (85%) was obviously higher than that of spherical ones (75%). These findings confirmed that the shapes of magnetic particles could generate a great impact on their interaction with CTCs and further affect the performance of magnetic screening.

In addition to particle size and shape, surface chemistry is another important property affecting the biological activities of micro-/nanomaterials.[76–78] The surface functional group, surface charge, and conjugation density have been demonstrated to significantly regulate the interactions between cells and particles. Although antibodies are always employed to modify the particle surface for recognizing specific tumor biomarkers, the detailed roles of surface chemistry of magnetic particles in liquid biopsies are rarely mentioned. By the aid of electrically charged magnetic nanoparticles, the effect of surface chemistry in CTCs screening was first revealed [Fig. 1(c)].[66] It was found that only positively charged particles were attached to cancer cells, while negatively charged ones did not. Positively charged particles offered a sensitivity

**TABLE I.** Recent progress of bulk techniques-enabled magnetic screening of circulating tumor biomarkers. ATF, amino-terminal fragment; HA, hyaluronan; PAH, poly(allylamine hydrochloride); PDs, polymer dots; PEI, polyethylenimine.

| Technique | Particle type | Particle source | Particle property | Surface conjugation | Biomarker type | Test object | Efficiency (%) | Reference (by year) |
|---|---|---|---|---|---|---|---|---|
| Photoacoustic | $Fe_2O_3$ | Ocean NanoTech | 10 nm; Sphere | ATF | MDAMB231cell | Tumor-bearing mice blood | >80 | 2009[33] |
| MagSweeper | Dynabeads | Invitrogen | Micrometers; sphere | Anti-HLA-A | Breast cancer cell | Patient blood | >50 | 2009[34] |
| Dynal MPC-s | Dynabeads | Invitrogen | 2.8 $\mu$m; sphere | Anti-EpCAM | DLD1 cell | Patient blood | ~80 | 2012[35] |
| Magnet | $Fe_3O_4$ | Self-made | 80 nm; sphere | SP94 | HepG2 | Spiked in PBS | 75 | 2013[36] |
| quad-μNMR | Microbeads | Miltenyi Biotec | Micrometers; sphere | Anti-EGFR; anti-EpCAM, anti-HER2, antivimentin | CTC | Patient blood | 62 | 2013[37] |
| Magnetic scaffold | γ-$Fe_2O_3$ | Self-made | 376 nm; sphere; 34.9 emu/g | Anti-EpCAM | CTC | Patient blood | 100 | 2014[38] |
| Magnetic rack; membrane filtration | Microbeads | Tianjin Beisile | 3 $\mu$m; sphere | Anti-EpCAM | MCF7 cell | Spiked in human blood | >98 | 2014[39] |
| Magnet | Nanobeads | Ademtech | 200 nm; sphere | Pep10 | MCF7 cell | Spiked in cells mixture | >90 | 2014[40] |
| Magnet | ScreenMAG | Chemicell | 500 nm; sphere | Folate | Hela cell | Spiked in rat blood | ~100 | 2014[41] |
| Magnetic sifter | MagCellect | R&D Systems | Sphere | Anti-EpCAM | Lung cancer cell | Patient blood | 50 | 2014[42] |
| Magnet | $Fe_3O_4$ | Self-made | ~10 nm; sphere | Aptamer | CCRF-CEM cells | Spiked in human blood | >70 | 2014[43] |
| Magnet | Dynabeads | Invitrogen | 2.8 $\mu$m; sphere | Aptamer | DLD1 cell | Spiked in human blood | 55 | 2015[44] |
| Magnet | $Fe_3O_4$ | Ocean NanoTech | 15 nm | Anti-EpCAM | SKBR3 cell | Spiked in mouse blood | 70–80 | 2015[45] |
| Magnet | Microbeads | Invitrogen | 2.8 $\mu$m; sphere | Anti-HER2 | SKBR3 cell | Spiked in mouse blood | >90 | 2015[46] |
| Magnet | $Fe_3O_4$-PDs | Self-made | ~40 nm; sphere; 32.6 emu/g | Anti-HER2 | SKBR3 cell | Spiked in rabbit blood | 97 | 2016[47] |
| Magnet | $Fe_3O_4$ | Self-made | ~200 nm; sphere; 18.76 emu/g | Anti-EpCAM | MCF-7 cell | Spiked in human blood | 85 | 2016[48] |
| Magnet | $Fe_3O_4$-lipid | Self-made | 219 nm; 42.3 emu/g | GE11 peptide | SMMC7721 cell | Patient blood | ~100 | 2016[49] |
| Magnet (neg) | γ-$Fe_2O_3$-Silica | Self-made | Sphere | Anti-CD45 | HCC cell | Patient blood | 100 | 2016[50] |
| Magnet | $Fe_3O_4$-tPG | Self-made | ~100 nm; sphere | Transferrin | HCT116 | Spiked in human blood | 33 | 2016[51] |
| Magnet | Dynabeads | Invitrogen | Micrometers; sphere | Anti-EpCAM | Lung cancer cell | Patient blood | 100 | 2016[52] |
| Magnet | MagneHis Ni; Ni-TAN | Promega; Taiwan Advanced NanoTech | Sphere | Annexin A5 | Exosome | Tumor-bearing mice blood | 50 | 2016[53] |
| Magnet | $Fe_3O_4$ | Sigma Aldrich | 30 nm | Anti-MCSP | LMMEL33 cell | Spiked in human blood | ~100 | 2017[54] |
| Magnet | $Fe_3O_4$-Silica | Self-made | 100–300 nm; sphere, rod; ~40–60 emu/g | Anti-EpCAM | Breast cancer cell | Patient blood | 75–85 | 2018[55] |
| Magnet | $Fe_3O_4$-QD | Ocean NanoTech | 15 nm; sphere | Aptamer | CCRF-CEM cell | Spiked in human blood | ~80 | 2018[56] |
| Magnetic wire | Nanobeads | N/A | Sphere | Anti-EpCAM | H1650 | Porcine blood | 100 | 2018[57] |
| Magnet | $Fe_3O_4$-tPG | Self-made | ~100–200 nm; sphere | Transferrin | HCT116 | Spiked in human blood | 13–81 | 2018[58] |
| Magnet | Nanobeads | Ocean NanoTech | 50 nm; sphere | Folate | SKOV3 cell | Spiked in cells mixture | ~70 | 2018[59] |

TABLE I. (*Continued.*)

| Technique | Particle type | Particle source | Particle property | Surface conjugation | Biomarker type | Test object | Efficiency (%) | Reference (by year) |
|---|---|---|---|---|---|---|---|---|
| Magnet | $Fe_3O_4$-Ppy | Self-made | 0.2 × 18 $\mu$m; wire | Anti-EpCAM, antivimentin, PEI | cfDNA; lung cancer cell | Patient blood | >70 | 2018[60] |
| Magnet | $Fe_2O_3$-graphene oxide | Self-made | Sheet | FGFR2:FAM76A fusion gene | ctRNA | Patient blood | 100 (1.0 fM) | 2018[61] |
| Magnet | $Fe_3O_4$-QD-$MoS_2$ | Self-made | ~12 nm | Anti-EpCAM | HepG2 cell | Spiked in human blood | 90 | 2019[62] |
| Magnet | $Fe_3O_4$ | Ocean NanoTech | 25 nm, 150 nm, 1 $\mu$m; sphere | Anti-EpCAM | MCF7 cell | Spiked in K562 cells | 60–80 | 2019[63] |
| Magnet | $Fe_3O_4$@HA | Self-made | 190 nm; 59 emu/g | Anti-EpCAM | CTC | Patient blood | >88 | 2019[64] |
| Magnet | $Fe_3O_4$-PAH-QD-HA | Self-made | 301 nm; sphere; 57.38 emu/g | Anti-EpCAM | CTC | Patient blood | 100 | 2019[65] |
| Magnet | $Fe_3O_4$@Silica | Self-made | 450 nm; sphere | PEI | Breast cancer cell | Patient blood | 100 | 2019[66] |
| Magnet | $Fe_3O_4$@Silica-FePt | Self-made | ~200 nm; sphere | tLyP-1 | HepG2 cell | Spiked in L02 cells | ~50–60 | 2019[67] |
| Magnet | $Fe_3O_4$-Ppy | Self-made | 0.2 × 18 $\mu$m; wire; 57 emu/g | Anti-CD9, anti-CD63, anti-CD81 | Exosome | Patient blood | 100 | 2019[68] |

of down to 4 CTCs in 1 ml blood samples and achieved a superior capture yield (>70%). In addition, the capture number of CTCs by positively charged particles from S180-bearing mice (75.8 CTCs per 100 $\mu$l blood) was significantly higher than that from healthy controls (0 CTCs per 100 $\mu$l blood), providing important guidelines for the rational design of particle surface in liquid biopsies.

It is noted that, according to the surface nature of magnetic particles, the screening methods of CTCs can be categorized into positive selection and negative selection. The former one uses antibodies (such as anti-EpCAM or anti-HER2) corresponding to the surface antigens of tumor cells to be enriched. However, because of the heterogeneous nature of cancer, the target CTCs may not all express the same antigens, and the potential influence of magnetic particles for downstream analysis is also one controversial issue. Therefore, negative selection methods that capture the blood cell and elute CTCs have been introduced [Fig. 1(d)], and anti-CD45 antibody is usually used since it is a standard protein criterion expressed on the surface of leukocytes.[50]

Although CTCs have provided great insights into cancer progression and a majority of studies in circulating tumor biomarkers screening focused on CTCs as discussed above, identification and enumeration of this kind of rare biomarker using magnetic approaches is technically challenging because of their exceeding rarity in the bloodstream. Alternatively, some studies, although very few, have been devoted to the magnetic screening of other circulating tumor biomarkers such as exosomes and nucleic acids.

Circulating tumor exosomes are membrane-bound phospholipid vesicles that are actively secreted from cancer cells.[2] These extracellular vesicles contain a series of important biomolecules from their parent cells such as nucleic acids and proteins, which make them useful for cancer diagnosis. Although exosomes hold great promise for liquid biopsies, there are very few studies exploring the interactions of exosomes with magnetic particles. When spherical magnetic beads were conjugated with annexin A5 (ANX-beads) that specifically bound to phosphatidylserine moieties on the surface of most extracellular vesicles, up to 60% of exosomes could be successfully captured by the ANX-beads.[53] In addition, in rodents xenografted with human cancer cells, tumor-derived mRNA could be detected in exosomes captured from serum, while active proteins could be detected in exosomes captured from ascites but not from plasma. However, it was found that the use of antibody cocktail-conjugated magnetic nanowires result in approximately threefold greater capture yield of exosomes compared to conventional methods [Fig. 2(a)].[68] The elongated morphology of magnetic nanowires affords more flexibility and versatility for exosome screening by facilitating multiple interactions through recognition receptors on exosomes, thereby resulting in enhanced exosome recovery even from small volumes of blood plasma of cancer patients. These results not only demonstrate the feasibility of magnetic materials for exosomes screening but also highlight the rational design of particle shape and surface for more effective analysis.

Nucleic acids are information-rich and are involved in many critical biological processes. Most nucleic acids are located within cells, and a small amount of them can also be found circulating freely in plasma or serum.[2] By decoding the contained genetic and epigenetic information, circulating tumor cell-free DNA and RNA

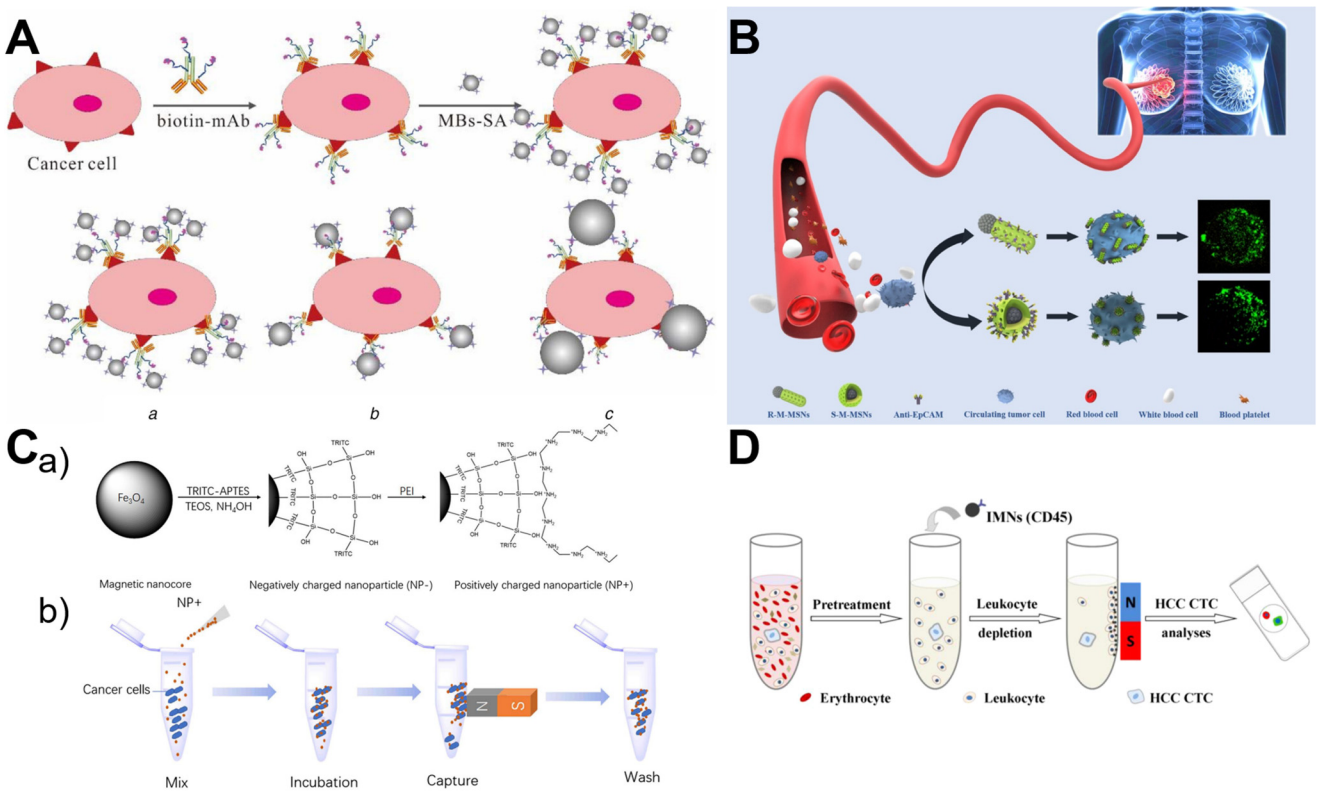


**FIG. 1.** Roles of particle size (a), shape (b), and surface functionalization [(c) and (d)] in the magnetic screening of tumor cells from bulk techniques. (a) Size effects of magnetic beads in circulating tumor cells magnetic capture based on streptavidin–biotin complexation. (a), (b), and (c) are 25 nm, 150 nm, and 1 $\mu$m sized magnetic beads labeled cell, respectively. Reproduced with permission from Li *et al.*, IET Nanobiotechnol. **13**, 6 (2019). Copyright 2019 Institute of Electrical and Electronics Engineers.[63] (b) Shape engineering (sphere and rod) boosts magnetic mesoporous silica nanoparticle-based isolation and detection of circulating tumor cells. Reproduced with permission from Chang *et al.*, ACS Appl. Mater. Interfaces **10**, 10656 (2018). Copyright 2018 American Chemical Society.[55] (c) Effective capture of circulating tumor cells from an S180-bearing mouse model using electrically charged magnetic nanoparticles. (a) Schematic diagram showing the design of surface-charged, fluorescent, superparamagnetic composite nanoparticles (NPs). (b) Illustration of the procedures for positive selection of cancer cells. Reproduced with permission from Li *et al.*, J. Nanobiotechnol. **17**, 59 (2019). Copyright 2019 BMC.[66] (d) Biofunctionalized magnetic nanospheres-based negative cell selection strategy for efficient isolation of heterogeneous circulating hepatocellular carcinoma cells. Reproduced with permission from Chen *et al.*, Biosens. Bioelectron. **85**, 633 (2016). Copyright 2016 Elsevier.[50]

can be utilized as important tools to guide cancer theranostics. Using positively charged magnetic polypyrrole nanowire, cell-free DNA was found to be directly extracted from plasma samples of patients with lung cancer [Fig. 2(b)]. Owing to the strong electrostatic binding and condensation of negatively charged DNA induced by cationic polyethylenimine on nanowire surface, black particlelike structures could be seen clearly even with the naked eye upon addition of magnetic nanowires to plasma.[60] Relying on the electrocatalytic activity of graphene-loaded iron oxide nanoparticles (GO-NP$Fe_2O_3$), FGFR2:FAM76A fusion gene in circulating tumor RNA extracted from ovarian cancer patients were also successfully detected [Fig. 2(c)]. Such an amplification-free assay could achieve an excellent detection sensitivity down to 1.0 fM, high specificity, and excellent reproducibility (less than 5% RSD).[61] These findings provide important guidelines to design new functional magnetic materials with enhanced screening and detection efficiency of circulating nucleic acids.

## III. EMERGING ROLES OF MICROFLUIDICS IN MAGNETIC NANOPARTICLES SYNTHESIS AND MAGNETIC SCREENING OF CIRCULATING TUMOR BIOMARKERS

### A. Microfluidic reactors for magnetic materials synthesis

Compared to conventional flask-based batch reactors [Fig. 3(a)], microfluidic reactors [microreactors, Figs. 3(b) and 3(c)] could enable precise spatiotemporal manipulation of experimental parameters (such as flow rate, temperature, pressure, and microchannel dimensions), and thus provide a promising platform for the continuous synthesis of magnetic nanoparticles with unprecedented control over their size, shape, and surface properties. To date, microfluidic techniques have already demonstrated their great potentials in the rational design and controllable synthesis of a series of magnetic nanomaterials (Table II), including pure metals (such as Fe, Co, and Ni), iron oxides (such as $\alpha$-$Fe_2O_3$, $\gamma$-$Fe_2O_3$, and $Fe_3O_4$), and alloys (such as FeCo, FeMn, and CoSm).

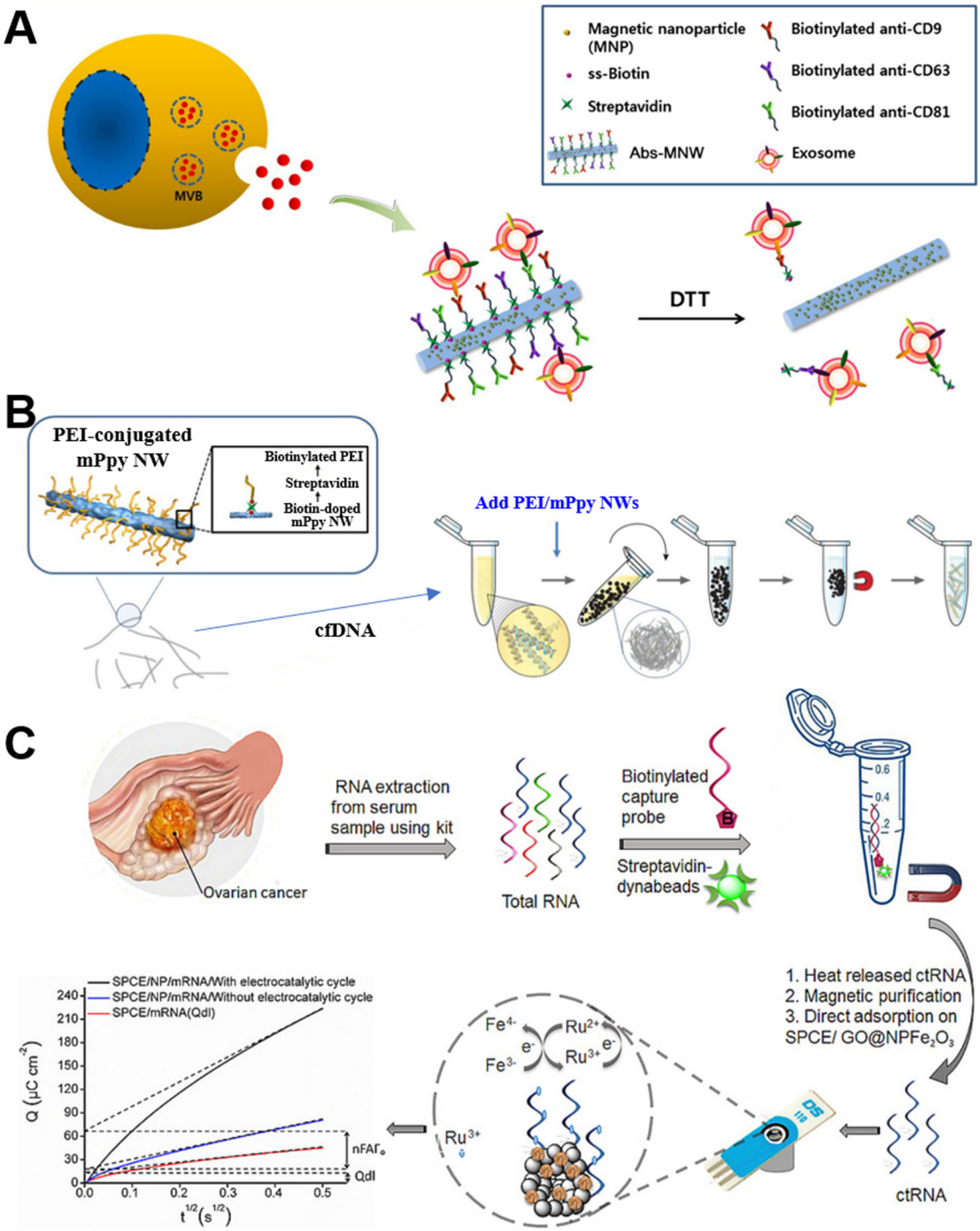


**FIG. 2.** Structural control of magnetic particles for circulating tumor exosomes (a), cfDNA (b), and ctRNA (c) screening from bulk techniques. (a) An illustration showing the antibody cocktail-conjugated magnetic nanowires used for the isolation of circulating exosomes. Reproduced with permission from Lim *et al.*, J. Nanobiotechnol. **17**, 1 (2019). Copyright 2019 BMC.[68] (b) Polyethylenimine-functionalized magnetic nanowire networks for ultrasensitive isolation and analysis of circulating tumor-specific cell-free DNA. Reproduced with permission from Li *et al.*, Theranostics **8**, 505 (2018). Copyright 2018 Ivyspring International Publisher.[60] (c) Detection of FGFR2:FAM76A fusion gene in circulating tumor RNA based on catalytic signal amplification of graphene oxide-loaded magnetic nanoparticles. Reproduced with permission from Gorgannezhad *et al.*, Electroanalysis **30**, 2293 (2018). Copyright 2018 Wiley.[61]

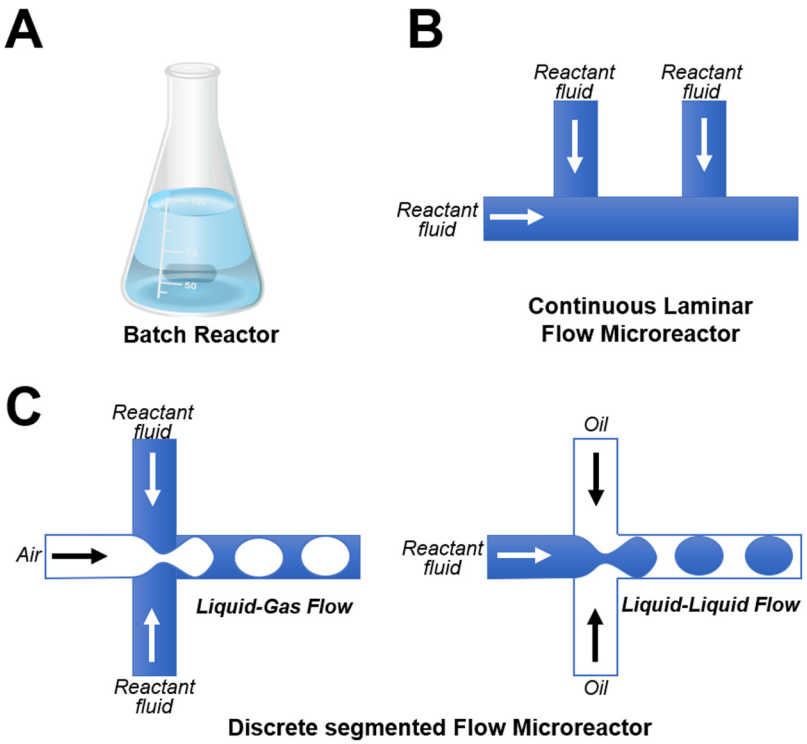


**FIG. 3.** Schematic illustrations showing different types of reactors for magnetic materials synthesis.

Generally, microreactors for magnetic materials synthesis can be broadly categorized into two groups: continuous laminar flow reactors [Fig. 3(b)] and discrete segmented flow reactors [Fig. 3(c)]. The former one involves only simple single phase aqueous fluids with multiple inlets for different reactants, special mixing module for diffusion-limited mixing, and one outlet for product collection. The latter one usually includes several aqueous fluids for the reactants and one gas/oil phase for the isolation of aqueous flows, which provides an enclosed compartment where reactants can mix dramatically with each other.[106,107]

Owing to relatively simple design and easy operation, continuous laminar flow microreactors are largely to be employed for the synthesis of magnetic materials with different size, shape, surface, and composition. For example, based on micropatterned plates [Fig. 4(a)], iron oxide nanoparticles with ultrasmall size (<4 nm) were produced by polyol-based pyrolysis method at high temperature (>200 °C) with short resident time (<1 min).[102] Using the Hastelloy tube reactor [Fig. 4(b)], PEGylated $Fe_3O_4$ nanoparticles (4.6 nm) could be directly prepared by pyrolysis method at 250 °C under pressure of 33 bar.[98] Similarly, Co nanoparticles (~4 nm) and Ni nanoparticles (5–10 nm) could be directly obtained via solution phase reduction and polyol-based solvothermal reduction, respectively [Figs. 4(c) and 4(d)].[80,93] In addition, the mixing, nucleation, growth, and termination stages during nanoparticles formation could be integrated through simple programmed microfluidic process [Fig. 4(e)], which provides a general approach for the synthesis of magnetic Fe, Co, Ni, CoFe, and NiFe materials with uniform sizes of less than 5 nm.[97] However, it is noted that almost all these studies reported small-sized spherical nanoparticles, shape control of magnetic nanoparticles through laminar flow microreactors is still a big challenge. Recently, using spiral-shaped laminar flow microreactor, we first created sphere-, ellipsoid-, rod-, and belt-shaped iron oxides by simply changing the flow rates and also developed robust methods to form core-shell and other kinds of magnetic-silica hybrids.[103–105]

Compared to continuous laminar flow microreactors, discrete segmented flow microreactors that permit more rapid and intensive mixing have attracted considerable attention from researchers. Structural control of discrete segmented flow microreactors is usually realized by droplet-based liquid-liquid phase separation. For example, the reactants in the droplet pairs could be brought together on demand by in-line electrocoalescence [Fig. 5(a)], which results in fast mixing (ca. 2 ms) and small-sized iron oxide nanoparticles (4 nm).[81] Through droplet- and ionic liquid-assisted microfluidic synthesis method, rod-shaped β-FeOOH (40 × 400 nm) was synthesized in only "20 min" of reaction time with a simple instrument [Fig. 5(b)].[90] Similarly, dextran-coated superparamagnetic iron oxide nanoparticles (3.6 nm) were directly obtained using capillary-based droplet microreactor [Fig. 5(c)].[92] In addition, recombinant *Escherichia coli* cell extracts-based biogenic approach was also developed to successfully synthesize magnetic FeMn [Fig. 5(d)] and $Fe_3O_4$ nanoparticles [Fig. 5(e)].[91,95] Comparatively, only a few studies reported on the liquid-gas phase separation methods for magnetic nanoparticle synthesis. Based on double-loop rotary micromixer that uses air microchannels connecting the membranes of every loop [Fig. 5(f)], it was found that size distribution of the resultant $Fe_3O_4$

**TABLE II.** Recent progress of microfluidics-enabled magnetic nanoparticles synthesis.

| Microreactor type | Particle type | Size | Shape | Monodispersity | Saturation magnetization | Reference (by year) |
|---|---|---|---|---|---|---|
| Glass capillary reactor | $\alpha$-$Fe_2O_3$ | 10–60 nm | Irregular | Low | N/A | 2005[79] |
| Y-shaped mixer | $\alpha$-/$\beta$-/$\varepsilon$-Co | 3.5–4.7 nm | Sphere | High | 39–142 emu/g | 2006[80] |
| Electrocoalescence droplet reactor | $Fe_3O_4$; $\gamma$-$Fe_2O_3$ | 4 nm | Sphere | High | $\sim 10^6$ A/m | 2008[81] |
| Coaxial flow capillary device | $\gamma$-$Fe_2O_3$ | 7 nm | Irregular | Medium | $1.4 \times 10^5$ A/m | 2008[82] |
| Y-shaped mixer | $\alpha$-/$\beta$-/$\varepsilon$-Co | ~2–4 nm | Sphere | High | N/A | 2008[83] |
| T-junction droplet reactor | $\gamma$-$Fe_2O_3$-hydrogel | ~30–40 $\mu$m | Sphere; disk; plug | High | $3.7 \times 10^5$ A/m | 2008[84] |
| Y-shaped mixer | CoSm | ~5 nm | Sphere | High | ~30 emu/g | 2009[85] |
| Double-loop micromixer | $Fe_3O_4$ | 4.83–6.69 nm | Irregular | High | 7 emu/g | 2009[86] |
| Y-shaped mixer | $\alpha$-/$\beta$-/$\varepsilon$-Co | 3.5–4.7 nm | Sphere | High | 1.5–155 emu/g | 2009[87] |
| Coaxial flow mixer | $\gamma$-$Fe_2O_3$@$SiO_2$ | 50 nm | Sphere | Low | N/A | 2009[88] |
| Coaxial flow mixer | $\beta$-FeOOH | ~7 nm | Irregular | Low | N/A | 2009[89] |
| T-junction droplet reactor | $\beta$-FeOOH | 40 × 400 nm | Rod | Medium | N/A | 2011[90] |
| Flow-focusing droplet reactor | $Fe_3O_4$ | 4.42 nm | Irregular | High | N/A | 2012[91] |
| Capillary-based droplet reactor | $Fe_3O_4$-dextran | 3.6 nm | Irregular | Medium | 58 emu/g | 2012[92] |
| T-shaped mixer | Ni | 5.4–9.2 nm | Irregular | High | 5.1 emu/g | 2012[93] |
| Y-shaped mixer | Co | 30 nm | Sphere | High | N/A | 2012[94] |
| Flow-focusing droplet reactor | FeMn | ~5 nm | Irregular | Low | ~1 emu/g | 2012[95] |
| Flow-focusing reactor | $Fe_3O_4$-alginate | 211–364 $\mu$m (diameter) | Fiber | High | 8 emu/g | 2012[96] |
| Y-shaped mixer | CoFe; Co; Fe; Ni; NiFe | <5 nm | Sphere | High | N/A | 2014[97] |
| T-shaped mixer | $Fe_3O_4$-PEG | 4.6 nm | Sphere | High | N/A | 2015[98] |
| T-shaped mixer | Ni | 15–83 nm | Sphere | Medium | N/A | 2015[99] |
| T-shaped mixer | $Fe_3O_4$; $\gamma$-$Fe_2O_3$ | 10 nm | Irregular | Low | 67.18 emu/g | 2017[100] |
| T-shaped mixer | $Co_3O_4$@$SiO_2$ | ~165 nm | Sphere | Medium | N/A | 2017[101] |
| Meandering-Spiral microchannel | $Fe_3O_4$ | <4 nm | Irregular | Medium | 24–64 emu/g | 2018[102] |
| Spiral microchannel | $\alpha$-$Fe_2O_3$ | ~20–350 nm | Sphere; cube; rod; belt | High | 5–10 emu/g | 2018[103] |
| Spiral microchannel | FeCo-Silica | ~2 $\mu$m | Flower | Medium | 13 emu/g | 2018[104] |
| Spiral microchannel | $Fe_3O_4$-$SiO_2$ | 1.2 $\mu$m | Sphere | High | N/A | 2019[105] |

nanoparticles is superior to that of batch systems even without requiring any extra heating or additives.[86] However, although these studies successfully demonstrated the feasibility of discrete segmented flow microreactors for the structural control of magnetic nanoparticles, continuous efforts are needed to precisely manipulate particle size, shape, and surface properties of magnetic materials for meeting diverse needs of liquid biopsies.

### B. Microfluidic chips for magnetic screening of circulating tumor biomarkers

Although great progress has been achieved in the field of bulk techniques-enabled magnetic screening of circulating tumor biomarkers (Table I), the efficiency, accuracy, and sensitivity issues are becoming more and more challenging. With the recent advancement of micro-/nanofabrication techniques, researchers are able to make miniaturized tools to manipulate extremely small objects in an efficient, flexible, customizable, reliable, and timely manner. For circulating tumor biomarkers screening, microfluidic systems could provide precise control of flow behavior and biological interactions within the microchannel settings.[2] Therefore, integration of the strengths of microfluidics for rare biomarkers handling with the benefits of immunomagnetic-based analysis has been well pursed for liquid biopsies in the last decade (Table III).

For the magnetic screening of circulating tumor cells, similar to conventional bulk techniques, microchip-based immunomagnetic assay utilizes magnetic particles that are conjugated with specific antibodies to label target cells and then applies an external magnetic field for capturing. To date, while plenty of studies have demonstrated superior capabilities of microfluidic techniques toward enhanced magnetic screening of CTCs (Table III), there is a lack of research into how structural properties of magnetic materials affect their screening performance. In the case of particle size effect, although many studies employed nano-/microsized magnetic beads/particles for tumor cells capture and analysis through microchips (Table III), the relevance of particle size with CTCs screening is still not yet revealed. In addition, almost all studies reported the spherical-shaped magnetic materials, nonspherical ones that hold great promise for improving the screening efficiency have received little attention. Recently, our group first developed a microfluidics-enabled strategy for the controllable synthesis of immunomagnetic nanomaterials with different shapes (sphere, cube, rod, and belt)

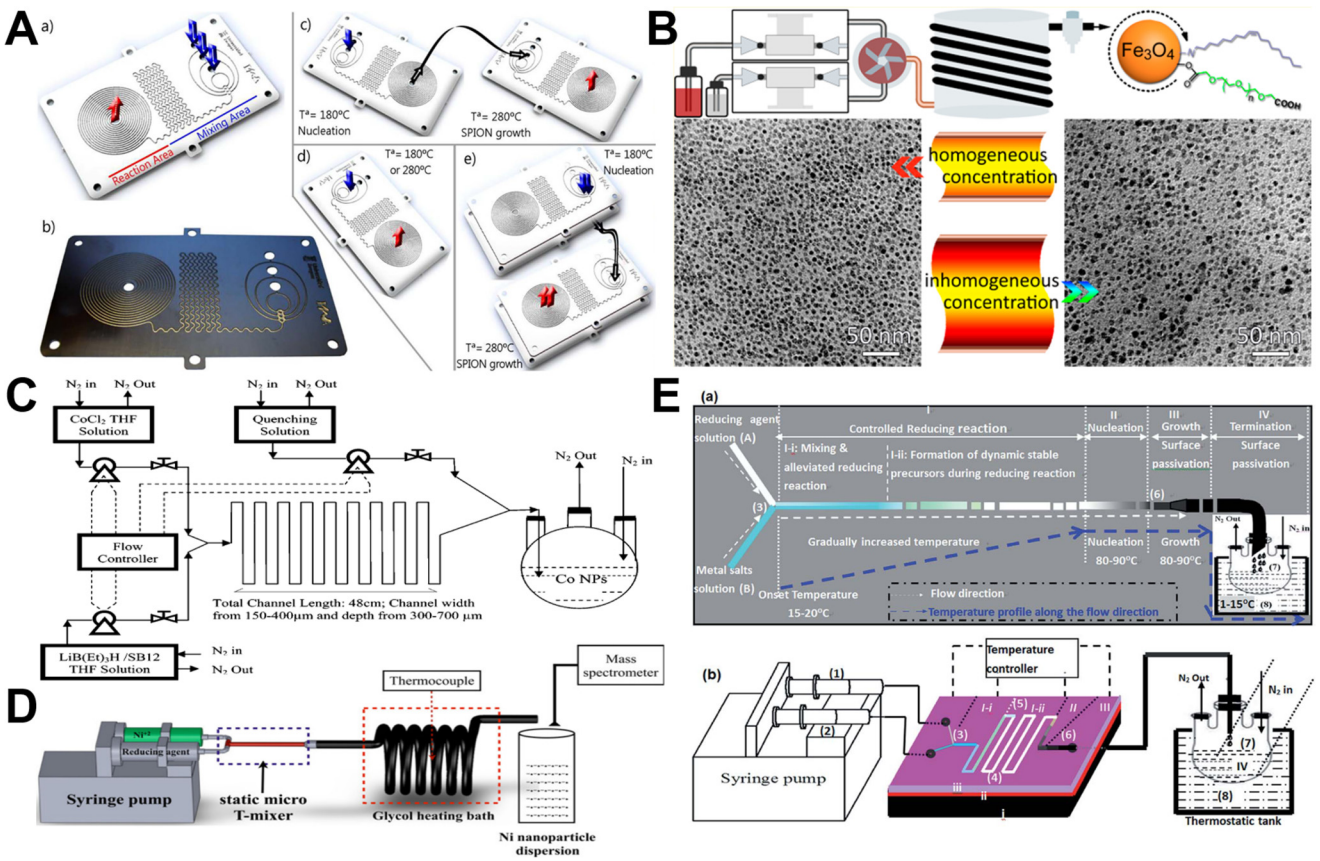


**FIG. 4.** Continuous laminar flow microreactors for the synthesis of magnetic nanomaterials. (a) Single phase microreactor for the continuous, high-temperature synthesis of <4 nm superparamagnetic iron oxide nanoparticles. Reproduced with permission from Uson *et al.*, Chem. Eng. J. **340**, 66 (2018). Copyright 2018 Elsevier.[102] (b) Flow synthesis of PEGylated $Fe_3O_4$ nanoparticles upon the pyrolysis of ferric acetylacetonate in anisole at 250 °C under pressure of 33 bar. Reproduced with permission from Jiao *et al.*, Chem. Mater. **27**, 1299 (2015). Copyright 2015 American Chemical Society.[98] (c) Schematic of the microfluidic reactor process for phase-controlled synthesis of cobalt nanoparticles. Reproduced with permission from Song *et al.*, Chem. Mater. **18**, 2817 (2006). Copyright 2006 American Chemical Society.[80] (d) Experimental setup used in continuous synthesis of nickel nanoparticles by hydrazine reduction. Reproduced with permission from R. Eluri and B. Paul, J. Nanopart. Res. **14**, 800 (2012). Copyright 2012 Springer Nature.[93] (e) Spatiotemporal-resolved magnetic nanoparticle synthesis via simple transparent chip-based simple programmed microfluidic processes (C-SPMPs). Reproduced with permission from Shen *et al.*, RSC Adv. **4**, 34179 (2014). Copyright 2014 Royal Society of Chemistry.[97]

and investigated the effect of particle shape on the screening efficiency of CTCs using our developed microchip [Fig. 6(a)]. We found that belt-shaped magnetic nanoparticles having the largest aspect ratio exhibited the highest capture rates in tumor cells-spiked whole blood samples, followed by rod-shaped nanoparticles, and sphere- and cube-shaped nanoparticles exhibited the relatively lowest capture efficiencies.[103] In another study, we fabricated hierarchical magnetic-silica microflower and investigated the direct interactions between microflower and tumor cells due to the easily recognizable particle shape under electron microscopy [Fig. 6(b)]. The results showed that cancer cell capture efficiency of such a hierarchical immunomagnetic system is significantly increased compared to standard CellSearch assay.[104] These findings bring new insights into the shape design of functional magnetic materials in liquid biopsies. In addition to particle size and shape, surface chemistry is another important parameter that needs to be considered adequately. Microchips-based immunomagnetic assays work either in a retaining mode (where CTCs are captured and fixed on the substrate) or in a depletion mode (where CTCs are driven to different streamlines and then be collected at outlet).[4] The former positive selection approach always uses anti-EpCAM to enrich tumor cells (Table III). However, as discussed above, the heterogeneous and mutagenic features of tumor cells could affect their biological properties, and thus an ideal CTC platform should not depend on subjective antigen expression. Therefore, considerable effort has been devoted to the latter negative selection approach that relies on the conjugation of anti-CD45 to magnetic particle surface [Figs. 6(c) and 6(d)].[110,114,122,125,129] However, it should be noted that negative selection may cause the loss of rare tumor cells during multiple processing procedures, and thus a combination of both position selection and negative selection is highly desired for achieving high screening efficiency.

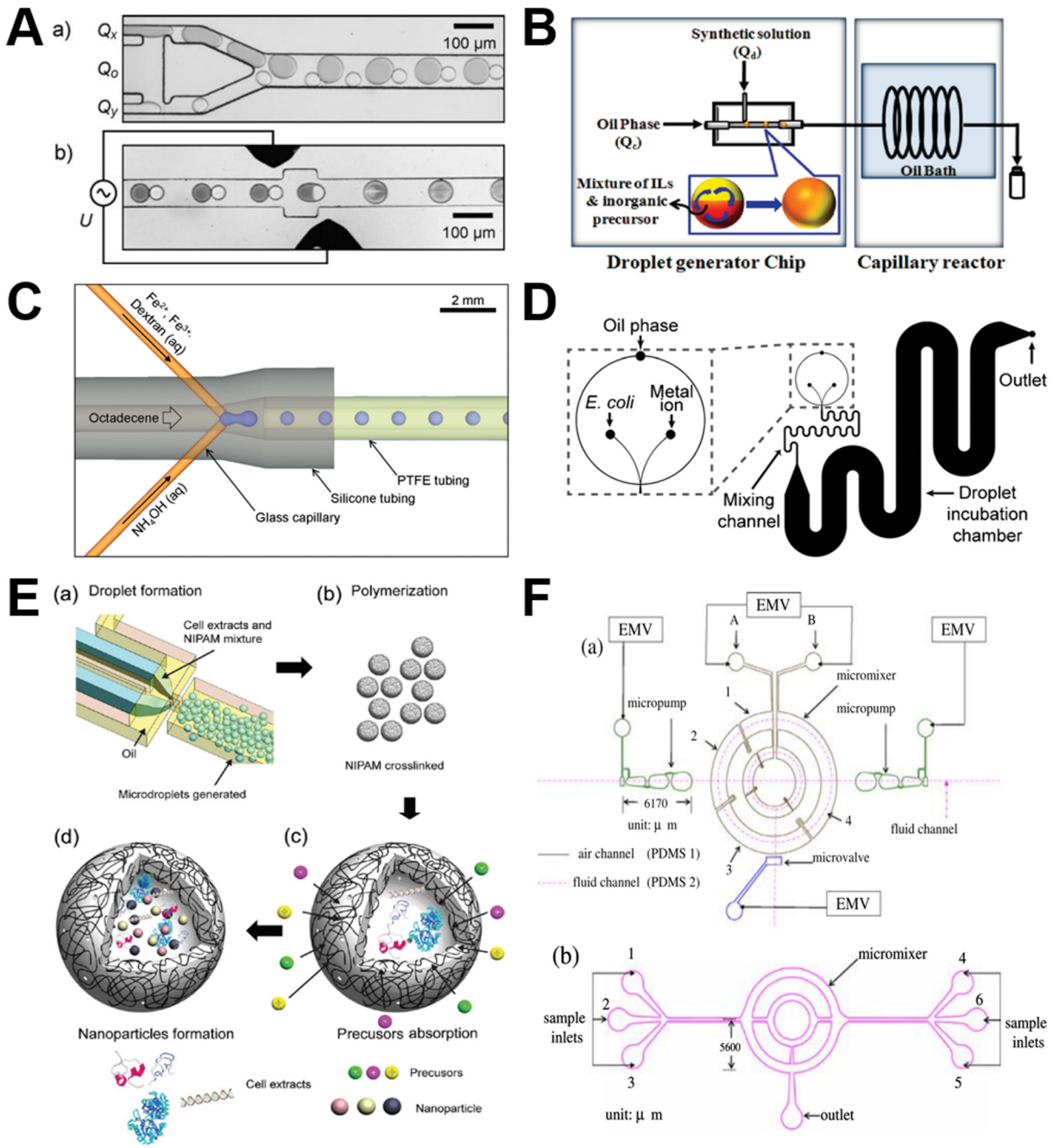


**FIG. 5.** Discrete segmented flow microreactors for the synthesis of magnetic nanomaterials. (a) Droplet-based microreactors for the synthesis of magnetic iron oxide nanoparticles by electrocoalescence pairing. Reproduced with permission from Frenz *et al.*, Angew. Chem. Int. Ed. **47**, 6817 (2008). Copyright 2008 Wiley.[81] (b) Synthesis of magnetic nanomaterials in droplet- and ionic liquid-assisted microfluidic system. Reproduced with permission from Hoang *et al.*, J. Am. Chem. Soc. **133**, 14765 (2011). Copyright 2011 American Chemical Society.[90] (c) Schematic of the capillary-based droplet reactor for the synthesis of iron oxide nanoparticles. Reproduced with permission from Kumar *et al.*, J. Mater. Chem. **22**, 4704 (2012). Copyright 2012 Royal Society of Chemistry.[92] (d) Design of the droplet microdevice for synthesizing biogenic magnetic FeMn nanoparticles. Reproduced with permission from Jung *et al.*, Angew. Chem. Int. Ed. **51**, 5634 (2012). Copyright 2012 Wiley.[95] (e) Schematic representation of the microdroplet-generation model using a microfluidic device for magnetic nanoparticle synthesis. Reproduced with permission from Li *et al.*, ACS Nano **6**, 6998 (2012). Copyright 2012 American Chemical Society.[91] (f) Schematic illustration of the double-loop micromixer for $Fe_3O_4$ nanoparticle synthesis. Reproduced with permission from Lee *et al.*, Biomed. Microdevices **11**, 161 (2009). Copyright 2009 Springer Nature.[86]

**TABLE III.** Recent progress of microfluidics-enabled magnetic screening of circulating tumor biomarkers. GBM, glioblastoma multiforme; iMER, immunomagnetic exosome RNA; MACS, magnetic-activated cell separation; MagRC, magnetic ranking cytometry; μNMR, micronuclear magnetic resonance; NSCLC, nonsmall-cell lung cancer; TEMPO, track etched magnetic micropore.

| Microchip type | Particle type | Particle source | Particle property | Surface conjugation | Biomarker type | Test object | Efficiency (%) | Reference (by year) |
|---|---|---|---|---|---|---|---|---|
| Micropillar array | Microbeads | Miltenyi Biotec | Micrometers; sphere | CD326 | SW620 cells | Spiked in PBS | 72.8 | 2011[108] |
| Parallel arrangement magnets | Ferrofluid | Veridex | ~10 nm | Anti-EpCAM | COLO205 cell; SKBR3 cell | Spiked in human blood | ~90 | 2011[109] |
| Multistage concentric-circular magnet (neg) | Microbeads | BD Biosciences | Sphere | Anti-CD45 | MCF7 cell | Spiked in mononuclear cells | 60 | 2011[110] |
| Micropillar array | Dynabeads | Invitrogen | 2.8 $\mu$m; sphere | Anti-EpCAM | 4T1 cell | Tumor-bearing mice blood | 100 | 2012[111] |
| μNMR | $Fe_3O_4$ | Self-made | 7 nm; sphere | Anti-CD63 | GBM microvesicle | Patient blood | 100 | 2012[112] |
| Parallel arrangement magnets | $Fe_3O_4$@Au | Self-made | 6.2 nm; sphere; 16.13 emu/g | Anti-EpCAM, anti-HER2, anti-EGFR | A431 cell; SKBR3 cell | Spiked in human blood | 93 | 2013[113] |
| Micropillar array; magnetophoresis (neg) | Dynal MyOne beads | Life Technologies | 1 $\mu$m; sphere | Anti-EpCAM, anti-CD45 | CTC | Patient blood | 100 | 2013[114] |
| Ephesia chip | Dynabeads | Invitrogen | 2.8 $\mu$m; sphere | Anti-EpCAM | MCF7 cell | Spiked in PBS | 65 | 2014[115] |
| Multistage cascading microchannel | Dynabeads | Invitrogen | 2.8 $\mu$m; sphere | Anti-IGF-1R | NSCLC exosome | Patient blood | 100 | 2014[116] |
| Silicon nanowire array | $NaYF_4$-$Fe_3O_4$-Au | Self-made | ~300 nm | Anti-EpCAM | Lung cancer cell | Patient blood | 100 | 2015[117] |
| Magnetic column; size-selective filter | $Fe_3O_4$ | Toda Kogyo Co. | 10 nm | None | GCIY-EGFP cell | Spiked in human blood | 80.7 | 2015[118] |
| Thin-film micromagnet | Ferrofluid | Janssen Diagnostic | ~10 nm | Anti-EpCAM | COLO205 cell | Spiked in human blood | 98 | 2015[119] |
| iMER chip | Magnetic polystyrene beads | Spherotech | 3 $\mu$m; sphere | Anti-CD63, anti-EGFR | GBM microvesicle | Patient blood | 100 | 2015[120] |
| Micromagnet array | Ferrofluid | Janssen Diagnostic | ~10 nm | Anti-EpCAM | COLO205 cell | Spiked in human blood | 95.6 | 2016[121] |
| Magnetic array (neg) | Microbeads | Stemcell Technologies | 1 $\mu$m; sphere | Anti-CD45 | NCIH1975, SW48, PC3, MCF7 | Spiked in human blood | >80 | 2016[122] |
| ExoSearch chip | Dynabeads | Invitrogen | 2.8 $\mu$m; sphere | Anti-CA-125, anti-EpCAM, anti-CD24 | Ovarian cancer exosome | Patient blood | 100 | 2016[123] |
| Silicon nanowire array | $Fe_3O_4$@Silica | Self-made | ~100 nm; sphere; ~40 emu/g | Anti-EpCAM | MCF7 cell | Spiked in PBS | 90.3 | 2017[124] |
| TEMPO (neg) | Nanobeads | N/A | 50 nm | Anti-CD45 | Pancreatic cancer cell | Patient blood | ~92 | 2017[125] |
| Wavy-herringbone | Dynabeads | Invitrogen | Sphere | Anti-EpCAM | HCT116 cell | Spiked in human blood | 81–95 | 2017[126] |
| MagRC | Nanobeads | N/A | 50 nm | Anti-EpCAM | Prostate cancer cell | Patient blood | 100 | 2017[127] |
| Parallel arrangement magnets | FeCo-Silica | Self-made | ~2 $\mu$m; flower; 13 emu/g | Anti-EpCAM | MCF7 cell | Spiked in human blood | >85 | 2018[104] |

TABLE III. (Continued.)

| Microchip type | Particle type | Particle source | Particle property | Surface conjugation | Biomarker type | Test object | Efficiency (%) | Reference (by year) |
|---|---|---|---|---|---|---|---|---|
| Parallel arrangement magnets | $\alpha$-$Fe_2O_3$ | Self-made | ~20–350 nm; sphere, cube, rod, belt; 5–10 emu/g | Anti-EpCAM | MCF7 cell | Spiked in human blood | 40–95 | 2018[103] |
| Microellipse pillar array | Dynabeads | Invitrogen | 4.5 $\mu$m; sphere | Anti-EpCAM | CTC | Patient blood | >90 | 2019[128] |
| Micropost array; MACS | Microbeads | Miltenyi Biotec | Micrometers; Sphere | Anti-CD45 | Liver cancer cell | Patient blood | 100 | 2019[129] |
| Parallel arrangement magnets | Nanobeads | MicroMod | 25–40 nm; sphere; 0.9 emu/g | Anti-EpCAM | CTC | Patient blood | 100 | 2019[130] |

Compared to circulating tumor cells, relatively little attention has been given to screening exosomes and nucleic acids through microchips (Table III). Although circulating exosomes and nucleic acids hold promise as potential biomarkers of cancer diagnosis and therapy effectiveness, their isolation, identification, and quantification remain challenging in terms of heterogeneity, integrity, and purity. The established microfluidics-based exosome screening relied mainly on spherical microsized or nanosized magnetic particles.[112,116,120,123] Using commercial-available 2.8 $\mu$m immunomagnetic beads, microchips could enable quantitative isolation and multiplexed detection of exosomes directly from a minimally invasive amount of plasma samples (as low as tens of microliters) in ovarian cancer patients [Fig. 7(a)][123] and nonsmall-cell lung cancer patients [Fig. 7(b)].[116] When integrated microchip with a miniaturized micronuclear magnetic resonance system, glioblastoma multiforme (GBM) exosomes were successfully differentiated from nontumor host cell-derived exosomes, and the protein concentration of target exosomes could be quantified after labeled with 7 nm magnetic nanoparticles [Fig. 7(c)].[112] Similarly, microchip was applied to analyze mRNA levels of $O^6$-methylguanine DNA methyltransferase and alkylpurine-DNA-*N*-glycosylase in magnetic beads-enriched tumor exosomes obtained from blood samples of GBM patients [Fig. 7(d)].[120] These preliminary studies validated the feasibility of microchips-based immunomagnetic approaches in exosomes enrichment and analysis; however, there is still a long way to go as regards sensitivity, accuracy, and specificity.

## IV. CURRENT CHALLENGES AND FUTURE PERSPECTIVES

Liquid biopsy brings new insights into point-of-care cancer theranostics. The last decade has witnessed considerable improvement in the magnetic screening of circulating tumor biomarkers toward liquid biopsy. Magnetic materials with different size, shape, surface, and composition have been applied for the isolation and detection of circulating tumor cells, exosomes, and nucleic acids. Both conventional bulk techniques and newly emerged microfluidic techniques served as important tools in the rational design of magnetic materials and applications in liquid biopsy. Although great success has been achieved, many challenges still lie ahead and more continuous efforts are still needed to integrate advances into clinical practices.

From magnetic material design aspect, conventional batch reactors allow one to produce magnetic particles with various physicochemical properties,[18,20–22] and microfluidic reactors also emerged as a promising platform for the controllable synthesis of magnetic particles.[5] However, most of researchers only focused on the magnetic property and did not pay enough attention to the structural features of magnetic materials (Tables I and III). This needs more intensively research collaborations drew from materials science and biomedical engineering. Specifically, (1) magnetic particles with sizes ranging from a few nanometers to several micrometers have been utilized for biomarkers screening. However, very few studies paid attention to reveal the effect of particle size in the screening performance of circulating tumor biomarkers.[63] More efforts in this area may greatly help for improving the screening performance. (2) A majority of studies employed spherical-shaped magnetic particles, especially those from commercial

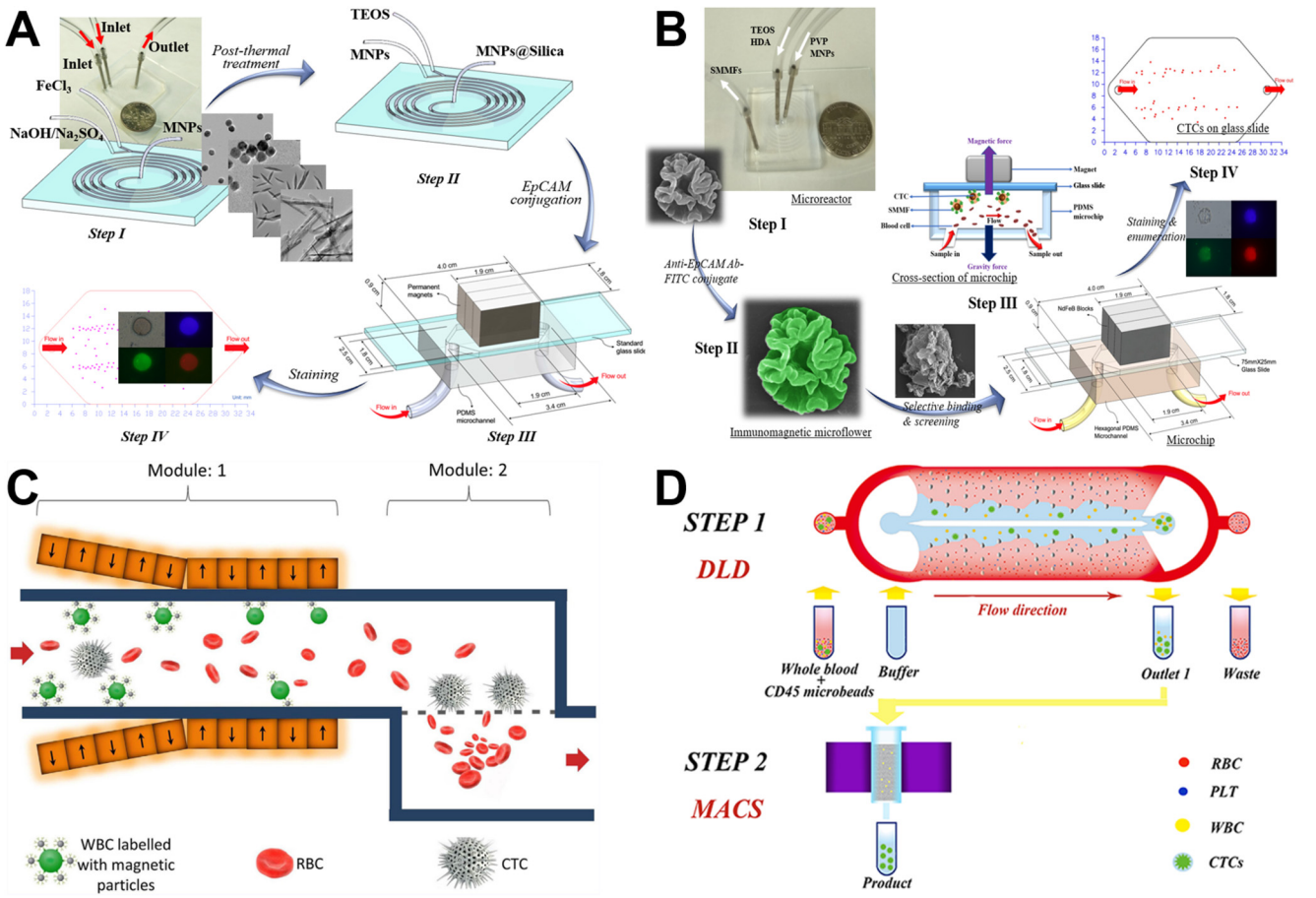


**FIG. 6.** Structural control of magnetic particles for circulating tumor cells screening from microfluidic techniques. (a) Microfluidics-enabled rational design of sphere-, cube-, rod-, and belt-shaped immunomagnetic nanomaterials and their shape effect on CTCs screening. Reproduced with permission from Hao *et al.*, Lab Chip **18**, 1997 (2018). Copyright 2018 Royal Society of Chemistry.[103] (b) Microfluidics-enabled rapid manufacturing of hierarchical silica-magnetic microflower toward enhanced circulating tumor cell screening. Reproduced with permission from Hao *et al.*, Biomater. Sci. **6**, 3121 (2018). Copyright 2018 Royal Society of Chemistry.[104] (c) An integrated on-chip platform for negative enrichment of tumor cells. Reproduced with permission from Bhuvanendran Nair Gourikutty *et al.*, J. Chromatogr. B **1028**, 153 (2016). Copyright 2016 Elsevier.[122] (d) Microfluidic chip combined with magnetic-activated cell sorting technology for tumor antigen-independent sorting of circulating hepatocellular carcinoma cells. Reproduced with permission from Wang *et al.*, PeerJ **7**, e6681 (2019). Copyright 2019 PeerJ.[129]

manufacturers. There is still no sufficient direct evidence to show a correlation between particle shape and tumor biomarkers screening.[55,103,104] Therefore, developing and examining nonspherical particles to improve the screening performance is still urgently required. (3) Although positive selection and negative selection methods have been widely used to recognize specific biomarkers, the evaluation on the surface characteristics of magnetic materials is still very simple. The conjugation density, stability, and target efficiency of antibodies should not be neglected, and more effective surface conjugation methods (such as antibody cocktail) can be employed. (4) Many studies only focused on the single composition (such as $Fe_3O_4$ or $Fe_2O_3$). The development of hierarchical hybrid structures such as magnetic-silica or magnetic-gold may not only improve the stability of magnetic particles but also provide great convenience for realizing downstream *in situ* analysis.[113,117]

From the biomarkers screening aspect, (1) a large number of studies have demonstrated the feasibility of conventional bulk techniques in the screening of circulating tumor cells, exosomes, and nucleic acids (Table I). Microfluidic chips also hold great promise for enhancing the screening efficacy toward liquid biopsy (Table III). Either positive retaining approach or negative depletion approach has been commonly applied in the magnetic screening of circulating tumor biomarkers. However, both approaches have shortcomings, and it is important that researchers are aware of these for developing more effective integrated approaches.[114] (2) From past and present studies, magnetic screening of tumor cells has attracted overwhelming attention from researchers due to the relatively easy isolation, identification, and analysis of cell objects. Although great progress has been made, circulating tumor cells from clinical samples are extremely rare (especially at an early stage of cancer) and large population of

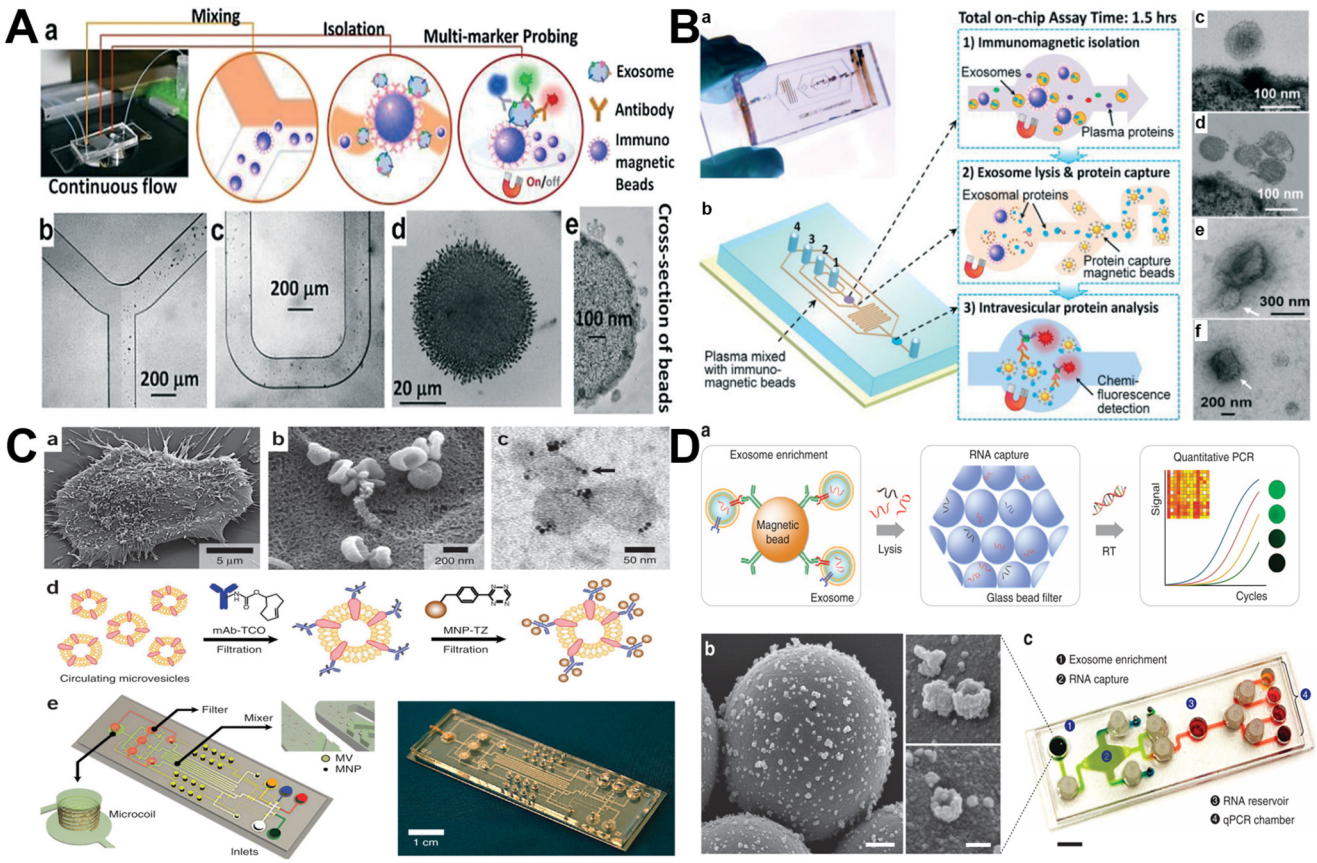


**FIG. 7.** Structural control of magnetic particles for circulating tumor exosomes screening from microfluidic techniques. (a) A microfluidic ExoSearch chip for multiplexed exosome detection towards blood-based ovarian cancer diagnosis. Reproduced with permission from Zhao *et al.*, Lab Chip **16**, 489 (2016). Copyright 2016 Royal Society of Chemistry.[123] (b) Integrated microfluidic exosome analysis directly from human plasma using microfluidic technology. Reproduced with permission from He *et al.*, Lab Chip **14**, 3773 (2014). Copyright 2014 Royal Society of Chemistry.[116] (c) μNMR-integrated microfluidic system for on-chip detection of circulating microvesicles (MV). Reproduced with permission from Shao *et al.*, Nat. Med. **18**, 1835 (2012). Copyright 2012 Springer Nature.[112] (d) Immunomagnetic exosomal RNA (iMER) platform-enabled exosome enrichment, RNA extraction, reverse transcription, and real-time analyses of distinct RNA targets in one small device. Reproduced with permission from Shao *et al.*, Nat. Commun. **6**, 6999 (2015). Copyright 2015 Springer Nature.[120]

background cells is present. Therefore, more robust, sensitive, and accurate assays need to be established for early point-of-care cancer theranostics. (3) Compared to circulating tumor cells, magnetic screening of circulating exosomes and nucleic acids still not received enough attention yet because of their relatively smaller sizes that need more precise and sophisticated measurement. This calls for more integrated tools from both materials and biomedical engineering fields to advance the applications of liquid biopsies.

From the microfluidics aspect, both magnetic nanomaterials synthesis and liquid biopsy applications have gained superior performance from microreactors (Table II) and microchips (Table III). To date, both continuous laminar flow reactors and discrete segmented flow reactors have already demonstrated their great potentials in the controllable synthesis of magnetic materials. Moving forward, precise control over particle size, shape, surface, and composition can be further explored using microfluidic reactors. Therefore, continuous efforts are required to systematically develop magnetic materials with tunable physicochemical properties. Similarly, although microchips hold great promise to improve the screening performance of circulating tumor biomarkers in terms of efficiency, accuracy, and sensitivity, most of microchip designs are only for the limited screening purpose (Figs. 6 and 7). Therefore, to fully exercise microfluidic systems, more integrated devices from upstream materials preparation to downstream biomarkers analysis can be developed for accelerating the translation of liquid biopsies into clinical practice.

## V. CONCLUSIONS

This review summarizes recent advances in magnetic materials for circulating tumor biomarkers screening in terms of rational design, microfluidic integration, and applications. We discussed conventional magnetic screening approaches in liquid biopsy, highlighted the newly emerged microfluidic techniques in both

controllable synthesis of magnetic materials through microreactors and magnetic screening applications of circulating tumor biomarkers through microchips, and finally pointed out the current challenges and opportunities for guiding future research. Given new breakthrough discoveries that are occurring in materials design and technique integration, we envision that magnetic materials-based bioassays will advance the fundamental understanding of circulating tumor biomarkers in liquid biopsy and translation for improving clinical outcomes.

## ACKNOWLEDGMENTS

The authors are grateful for the financial support from the National Institutes of Health (NIH) Director's Transformative Research Award No. (R01HL137157), NSF No. ECCS-1509369, and Norris Cotton Cancer Center Developmental Funds (Pilot Projects).

## REFERENCES

[1]Y. Zhang, X. Mi, X. Tan, and R. Xiang, Theranostics **9**, 491 (2019).
[2]N. Hao and J. X. J. Zhang, Sep. Purif. Rev. **47**, 19 (2018).
[3]Y. Zhu, K. Kekalo, C. Ndong, Y. Huang, F. Shubitidze, K. E. Griswold, I. Baker, and J. X. J. Zhang, Adv. Funct. Mater. **26**, 3953 (2016).
[4]P. Chen, Y. Huang, K. Hoshino, and X. Zhang, Lab Chip **14**, 446 (2014).
[5]N. Hao, Y. Nie, and J. X. J. Zhang, Int. Mater. Rev. **63**, 461 (2018).
[6]L. Capretto, D. Carugo, S. Mazzitelli, C. Nastruzzi, and X. Zhang, Adv. Drug Deliv. Rev. **65**, 1496 (2013).
[7]K. S. Elvira, X. Casadevall i Solvas, R. C. R. Wootton, and A. J. de Mello, Nat. Chem. **5**, 905 (2013).
[8]P. M. Valencia, O. C. Farokhzad, R. Karnik, and R. Langer, Nat. Nanotechnol. **7**, 623 (2012).
[9]G. M. Whitesides, Nature **442**, 368 (2006).
[10]N. Hao, Y. Nie, and J. X. J. Zhang, Biomater. Sci. **7**, 2218 (2019).
[11]N. Hao, Y. Nie, A. B. Closson, and J. X. J. Zhang, J. Colloid Interf. Sci. **539**, 87 (2019).
[12]N. Hao, Y. Nie, Z. Xu, and J. X. J. Zhang, J. Colloid Interf. Sci. **542**, 370 (2019).
[13]N. Hao, Y. Nie, and J. X. J. Zhang, ACS Sustain. Chem. Eng. **6**, 1522 (2018).
[14]N. Hao, Y. Nie, A. Tadimety, A. B. Closson, and J. X. J. Zhang, Mater. Res. Lett. **5**, 584 (2017).
[15]M. A. M. Gijs, F. Lacharme, and U. Lehmann, Chem. Rev. **110**, 1518 (2010).
[16]A.-H. Lu, E. L. Salabas, and F. Schüth, Angew. Chem. Int. Ed. **46**, 1222 (2007).
[17]S. Laurent, D. Forge, M. Port, A. Roch, C. Robic, L. Vander Elst, and R. N. Muller, Chem. Rev. **108**, 2064 (2008).
[18]N. A. Frey, S. Peng, K. Cheng, and S. Sun, Chem. Soc. Rev. **38**, 2532 (2009).
[19]J. Gao, H. Gu, and B. Xu, Acc. Chem. Res. **42**, 1097 (2009).
[20]W. Wu, Z. Wu, T. Yu, C. Jiang, and W.-S. Kim, Sci. Technol. Adv. Mater. **16**, 023501 (2015).
[21]R. Hao, R. Xing, Z. Xu, Y. Hou, S. Gao, and S. Sun, Adv. Mater. **22**, 2729 (2010).
[22]T. Hyeon, Chem. Commun. **39**, 927 (2003).
[23]N. Hao, Z. Xu, Y. Nie, C. Jin, A. B. Closson, M. Zhang, and J. X. J. Zhang, Chem. Eng. J. **378**, 122222 (2019).
[24]J. A. Champion, Y. K. Katare, and S. Mitragotri, J. Control. Release **121**, 3 (2007).
[25]N. Hao, L. L. Li, Q. Zhang, X. L. Huang, X. W. Meng, Y. Q. Zhang, D. Chen, F. Q. Tang, and L. F. Li, Micropor. Mesopor. Mater. **162**, 14 (2012).
[26]Y. Geng, P. Dalhaimer, S. S. Cai, R. Tsai, M. Tewari, T. Minko, and D. E. Discher, Nat. Nanotechnol. **2**, 249 (2007).
[27]N. Hao, L. F. Li, and F. Q. Tang, Int. Mater. Rev. **62**, 57 (2017).
[28]N. Hao, L. Li, and F. Tang, Biomater. Sci. **4**, 575 (2016).
[29]N. Hao, X. Chen, K. W. Jayawardana, B. Wu, M. Sundhoro, and M. Yan, Biomater. Sci. **4**, 87 (2016).
[30]N. Hao, F. Q. Tang, and L. F. Li, Micropor. Mesopor. Mater. **218**, 223 (2015).
[31]N. Hao, Y. Nie, and J. X. J. Zhang, Micropor. Mesopor. Mater. **261**, 144 (2018).
[32]N. Hao, H. T. Chorsi, and J. X. J. Zhang, ACS Sustain. Chem. Eng. **5**, 2044 (2017).
[33]E. I. Galanzha, E. V. Shashkov, T. Kelly, J.-W. Kim, L. Yang, and V. P. Zharov, Nat. Nanotechnol. **4**, 855 (2009).
[34]A. H. Talasaz, A. A. Powell, D. E. Huber, J. G. Berbee, K.-H. Roh, W. Yu, W. Xiao, M. M. Davis, R. F. Pease, M. N. Mindrinos, S. S. Jeffrey, and R. W. Davis, Proc. Natl. Acad. Sci. U.S.A. **106**, 3970 (2009).
[35]M. Gazouli, World J. Gastroenterol. **18**, 4419 (2012).
[36]Y. Wang, H.-Z. Jia, K. Han, R.-X. Zhuo, and X.-Z. Zhang, J. Mater. Chem. B **1**, 3344 (2013).
[37]A. A. Ghazani, S. McDermott, M. Pectasides, M. Sebas, M. Mino-Kenudson, H. Lee, R. Weissleder, and C. M. Castro, Nanomedicine **9**, 1009 (2013).
[38]C.-Y. Wen, L.-L. Wu, Z.-L. Zhang, Y.-L. Liu, S.-Z. Wei, J. Hu, M. Tang, E.-Z. Sun, Y.-P. Gong, J. Yu, and D.-W. Pang, ACS Nano **8**, 941 (2014).
[39]H. Zhang, Y. Wang, Q. Li, F. Zhang, and B. Tang, Chem. Commun. **50**, 7024 (2014).
[40]L. Bai, Y. Du, J. Peng, Y. Liu, Y. Wang, Y. Yang, and C. Wang, J. Mater. Chem. B **2**, 4080 (2014).
[41]W. Shi, R. J. Paproski, R. Moore, and R. Zemp, J. Biomed. Opt. **19**, 056014 (2014).
[42]C. M. Earhart, C. E. Hughes, R. S. Gaster, C. C. Ooi, R. J. Wilson, L. Y. Zhou, E. W. Humke, L. Xu, D. J. Wong, S. B. Willingham, E. J. Schwartz, I. L. Weissman, S. S. Jeffrey, J. W. Neal, R. Rohatgi, H. A. Wakelee, and S. X. Wang, Lab Chip **14**, 78 (2014).
[43]S. Fang, C. Wang, J. Xiang, L. Cheng, X. Song, L. Xu, R. Peng, and Z. Liu, Nano Res. **7**, 1327 (2014).
[44]C. Sun, R. Zhang, M. Gao, and X. Zhang, Anal. Bioanal. Chem. **407**, 8883 (2015).
[45]H. Min, S.-M. Jo, and H.-S. Kim, Small **11**, 2536 (2015).
[46]S.-M. Jo, J. Lee, W. Heu, and H.-S. Kim, Small **11**, 1975 (2015).
[47]A. Pramanik, A. Vangara, B. P. Viraka Nellore, S. S. Sinha, S. R. Chavva, S. Jones, and P. C. Ray, ACS Appl. Mater. Interfaces **8**, 15076 (2016).
[48]J. Wu, X. Wei, J. Gan, L. Huang, T. Shen, J. Lou, B. Liu, J. X. J. Zhang, and K. Qian, Adv. Funct. Mater. **26**, 4016 (2016).
[49]J. Ding, K. Wang, W.-J. Tang, D. Li, Y.-Z. Wei, Y. Lu, Z.-H. Li, and X.-F. Liang, Anal. Chem. **88**, 8997 (2016).
[50]L. Chen, L. L. Wu, Z. L. Zhang, J. Hu, M. Tang, C. B. Qi, N. Li, and D. W. Pang, Biosens. Bioelectron. **85**, 633 (2016).
[51]M. Asadian-Birjand, C. Biglione, J. Bergueiro, A. Cappelletti, C. Rahane, G. Chate, J. Khandare, B. Klemke, M. C. Strumia, and M. Calderón, Macromol. Rapid Commun. **37**, 439 (2016).
[52]C. E. Yoo, J.-M. Park, H.-S. Moon, J.-G. Joung, D.-S. Son, H.-J. Jeon, Y. J. Kim, K.-Y. Han, J.-M. Sun, K. Park, D. Park, and W.-Y. Park, Sci. Rep. **6**, 37392 (2016).
[53]C.-L. Shih, K.-Y. Chong, S.-C. Hsu, H.-J. Chien, C.-T. Ma, J. W.-C. Chang, C.-J. Yu, and C.-C. Chiou, New Biotechnol. **33**, 116 (2016).
[54]J. Li, J. Wang, Y. Wang, and M. Trau, Analyst **142**, 4788 (2017).
[55]Z. Chang, Z. Wang, D. Shao, J. Yue, H. Xing, L. Li, M. Ge, M. Li, H. Yan, H. Hu, Q. Xu, and W. Dong, ACS Appl. Mater. Interfaces **10**, 10656 (2018).
[56]Z. Li, G. Wang, Y. Shen, N. Guo, and N. Ma, Adv. Funct. Mater. **28**, 1707152 (2018).
[57]O. Vermesh, A. Aalipour, T. J. Ge, Y. Saenz, Y. Guo, I. S. Alam, S. Park, C. N. Adelson, Y. Mitsutake, J. Vilches-Moure, E. Godoy, M. H. Bachmann, C. C. Ooi, J. K. Lyons, K. Mueller, H. Arami, A. Green, E. I. Solomon, S. X. Wang, and S. S. Gambhir, Nat. Biomed. Eng. **2**, 696 (2018).
[58]C. Biglione, J. Bergueiro, M. Asadian-Birjand, C. Weise, V. Khobragade, G. Chate, M. Dongare, J. Khandare, M. Strumia, and M. Calderón, Polymers **10**, 174 (2018).

[59]F. Li, G. Yang, Z. P. Aguilar, Y. Xiong, and H. Xu, Sensor. Actuat. B **262**, 611 (2018).
[60]H. Lee, M. Choi, J. Lim, M. Jo, J.-Y. Han, T. M. Kim, and Y. Cho, Theranostics **8**, 505 (2018).
[61]L. Gorgannezhad, M. Umer, M. Kamal Masud, M. S. A. Hossain, S. Tanaka, Y. Yamauchi, C. Salomon, R. Kline, N.-T. Nguyen, and M. J. A. Shiddiky, Electroanalysis **30**, 2293 (2018).
[62]F. Cui, J. Ji, J. Sun, J. Wang, H. Wang, Y. Zhang, H. Ding, Y. Lu, D. Xu, and X. Sun, Anal. Bioanal. Chem. **411**, 985 (2019).
[63]F. Li, H. Xu, P. Sun, Z. Hu, and Z. P. Aguilar, IET Nanobiotechnol. **13**, 6 (2019).
[64]S. Ma, X. Zhou, Q. Chen, P. Jiang, F. Lan, Q. Yi, and Y. Wu, J. Colloid Interf. Sci. **545**, 94 (2019).
[65]X. Zhou, B. Luo, K. Kang, S. Ma, X. Sun, F. Lan, Q. Yi, and Y. Wu, J. Mater. Chem. B **7**, 393 (2019).
[66]Z. Li, J. Ruan, and X. Zhuang, J. Nanobiotechnol. **17**, 59 (2019).
[67]C. Liu, B. Yang, X. Chen, Z. Hu, Z. Dai, D. Yang, X. Zheng, X. She, and Q. Liu, Nanotechnology **30**, 285706 (2019).
[68]J. Lim, M. Choi, H. Lee, Y.-H. Kim, J.-Y. Han, E. S. Lee, and Y. Cho, J. Nanobiotechnol. **17**, 1 (2019).
[69]W. Zauner, N. A. Farrow, and A. M. R. Haines, J. Control. Release **71**, 39 (2001).
[70]K. Yin Win and S. S. Feng, Biomaterials **26**, 2713 (2005).
[71]F. Lu, S.-H. Wu, Y. Hung, and C.-Y. Mou, Small **5**, 1408 (2009).
[72]C. He, Y. Hu, L. Yin, C. Tang, and C. Yin, Biomaterials **31**, 3657 (2010).
[73]J. A. Champion and S. Mitragotri, Proc. Natl. Acad. Sci. U.S.A. **103**, 4930 (2006).
[74]S. E. A. Gratton, P. A. Ropp, P. D. Pohlhaus, J. C. Luft, V. J. Madden, M. E. Napier, and J. M. DeSimone, Proc. Natl. Acad. Sci. U.S.A. **105**, 11613 (2008).
[75]N. Hao, L. Li, and F. Tang, J. Biomed. Nanotechnol. **10**, 2508 (2014).
[76]I. Slowing, B. G. Trewyn, and V. S.-Y. Lin, J. Am. Chem. Soc. **128**, 14792 (2006).
[77]A. Verma and F. Stellacci, Small **6**, 12 (2010).
[78]T. S. Hauck, A. A. Ghazani, and W. C. W. Chan, Small **4**, 153 (2008).
[79]T. Miyake, T. Ueda, N. Ikenaga, H. Oda, and M. Sano, J. Mater. Sci. **40**, 5011 (2005).
[80]Y. Song, H. Modrow, L. L. Henry, C. K. Saw, E. E. Doomes, V. Palshin, J. Hormes, and C. S. S. R. Kumar, Chem. Mater. **18**, 2817 (2006).
[81]L. Frenz, A. El Harrak, M. Pauly, S. Bégin-Colin, A. D. Griffiths, and J. C. Baret, Angew. Chem. Int. Ed. **47**, 6817 (2008).
[82]A. Abou Hassan, O. Sandre, V. Cabuil, and P. Tabeling, Chem. Commun. **2008**, 1783.
[83]Y. Song, T. Zhang, W. Yang, S. Albin, and L. L. Henry, Cryst. Growth Des. **8**, 3766 (2008).
[84]D. K. Hwang, D. Dendukuri, and P. S. Doyle, Lab Chip **8**, 1640 (2008).
[85]Y. Song and L. L. Henry, Nanoscale Res. Lett. **4**, 1130 (2009).
[86]W.-B. Lee, C.-H. Weng, F.-Y. Cheng, C.-S. Yeh, H.-Y. Lei, and G.-B. Lee, Biomed. Microdevices **11**, 161 (2009).
[87]Y. Song, L. L. Henrys, and W. Yang, Langmuir **25**, 10209 (2009).
[88]A. Abou-Hassan, R. Bazzi, and V. Cabuil, Angew. Chem. Int. Ed. **48**, 7180 (2009).
[89]A. Abou-Hassan, J. F. Dufrêchfer, O. Sandre, G. Mériguet, O. Bernard, and V. Cabuil, J. Phys. Chem. C **113**, 18097 (2009).
[90]P. H. Hoang, H. Park, and D. P. Kim, J. Am. Chem. Soc. **133**, 14765 (2011).
[91]K. G. Lee, J. Hong, K. W. Wang, N. S. Heo, D. H. Kim, S. Y. Lee, S. J. Lee, and T. J. Park, ACS Nano **6**, 6998 (2012).
[92]K. Kumar, A. M. Nightingale, S. H. Krishnadasan, N. Kamaly, M. Wylenzinska-Arridge, K. Zeissler, W. R. Branford, E. Ware, A. J. DeMello, and J. C. DeMello, J. Mater. Chem. **22**, 4704 (2012).
[93]R. Eluri and B. Paul, J. Nanopart. Res. **14**, 800 (2012).
[94]L. Gomez, V. Sebastian, S. Irusta, A. Ibarra, M. Arruebo, and J. Santamaria, Lab Chip **14**, 325 (2014).
[95]J. H. Jung, T. J. Park, S. Y. Lee, and T. S. Seo, Angew. Chem. Int. Ed. **51**, 5634 (2012).
[96]Y. S. Lin, K. S. Huang, C. H. Yang, C. Y. Wang, Y. S. Yang, H. C. Hsu, Y. J. Liao, and C. W. Tsai, PLoS One **7**, e33184 (2012).
[97]X. Shen, Y. Song, S. Li, R. Li, S. Ji, Q. Li, H. Duan, R. Xu, W. Yang, K. Zhao, R. Rong, and X. Wang, RSC Adv. **4**, 34179 (2014).
[98]M. Jiao, J. Zeng, L. Jing, C. Liu, and M. Gao, Chem. Mater. **27**, 1299 (2015).
[99]L. Xu, C. Srinivasakannan, J. Peng, D. Zhang, and G. Chen, Chem. Eng. Process. **93**, 44 (2015).
[100]S. Lin, K. Lin, D. Lu, and Z. Liu, J. Environ. Chem. Eng. **5**, 303 (2017).
[101]A. Straß, R. Maier, and R. Güttel, Chem. Ing. Tech. **89**, 963 (2017).
[102]L. Uson, M. Arruebo, V. Sebastian, and J. Santamaria, Chem. Eng. J. **340**, 66 (2018).
[103]N. Hao, Y. Nie, T. Shen, and J. X. J. Zhang, Lab Chip **18**, 1997 (2018).
[104]N. Hao, Y. Nie, A. Tadimety, T. Shen, and J. X. J. Zhang, Biomater. Sci. **6**, 3121 (2018).
[105]N. Hao, Y. Nie, Z. Xu, A. B. Closson, T. Usherwood, and J. X. J. Zhang, Chem. Eng. J. **366**, 433 (2019).
[106]H. Song, D. L. Chen, and R. F. Ismagilov, Angew. Chem. Int. Ed. **45**, 7336 (2006).
[107]S.-Y. Teh, R. Lin, L.-H. Hung, and A. P. Lee, Lab Chip **8**, 198 (2008).
[108]C. Z. Zhou, Y. G. Li, X. Chen, Z. H. Peng, and J. Xia, IET Nanobiotechnol. **5**, 114 (2011).
[109]K. Hoshino, Y.-Y. Huang, N. Lane, M. Huebschman, J. W. Uhr, E. P. Frenkel, and X. Zhang, Lab Chip **11**, 3449 (2011).
[110]C.-L. Chen, K.-C. Chen, Y.-C. Pan, T.-P. Lee, L.-C. Hsiung, C.-M. Lin, C.-Y. Chen, C.-H. Lin, B.-L. Chiang, and A. M. Wo, Lab Chip **11**, 474 (2011).
[111]J. H. Kang, S. Krause, H. Tobin, A. Mammoto, M. Kanapathipillai, and D. E. Ingber, Lab Chip **12**, 2175 (2012).
[112]H. Shao, J. Chung, L. Balaj, A. Charest, D. D. Bigner, B. S. Carter, F. H. Hochberg, X. O. Breakefield, R. Weissleder, and H. Lee, Nat. Med. **18**, 1835 (2012).
[113]C. H. Wu, Y. Y. Huang, P. Chen, K. Hoshino, H. Liu, E. P. Frenkel, J. X. J. Zhang, and K. V. Sokolov, ACS Nano **7**, 8816 (2013).
[114]E. Ozkumur, A. M. Shah, J. C. Ciciliano, B. L. Emmink, D. T. Miyamoto, E. Brachtel, M. Yu, P. Chen, B. Morgan, J. Trautwein, A. Kimura, S. Sengupta, S. L. Stott, N. M. Karabacak, T. A. Barber, J. R. Walsh, K. Smith, P. S. Spuhler, J. P. Sullivan, R. J. Lee, D. T. Ting, X. Luo, A. T. Shaw, A. Bardia, L. V. Sequist, D. N. Louis, S. Maheswaran, R. Kapur, D. A. Haber, and M. Toner, Sci. Transl. Med. **5**, 179ra47 (2013).
[115]Z. Svobodova, J. Kucerova, J. Autebert, D. Horak, L. Bruckova, J. Viovy, and Z. Bilkova, Electrophoresis **35**, 323 (2014).
[116]M. He, J. Crow, M. Roth, Y. Zeng, and A. K. Godwin, Lab Chip **14**, 3773 (2014).
[117]C. Wang, M. Ye, L. Cheng, R. Li, W. Zhu, Z. Shi, C. Fan, J. He, J. Liu, and Z. Liu, Biomaterials **54**, 55 (2015).
[118]S. Yamamoto, J. Fei, M. Okochi, K. Shimizu, A. Yusa, N. Kondo, H. Iwata, H. Nakanishi, and H. Honda, Bioprocess Biosys. Eng. **38**, 1693 (2015).
[119]P. Chen, Y.-Y. Huang, K. Hoshino, and J. X. J. Zhang, Sci. Rep. **5**, 8745 (2015).
[120]H. Shao, J. Chung, K. Lee, L. Balaj, C. Min, B. S. Carter, F. H. Hochberg, X. O. Breakefield, H. Lee, and R. Weissleder, Nat. Commun. **6**, 6999 (2015).
[121]P. Chen, Y. Y. Huang, G. Bhave, K. Hoshino, and X. Zhang, Ann. Biomed. Eng. **44**, 1710 (2016).
[122]S. Bhuvanendran Nair Gourikutty, C.-P. Chang, and D. P. Poenar, J. Chromatogr. B **1028**, 153 (2016).
[123]Z. Zhao, Y. Yang, Y. Zeng, and M. He, Lab Chip **16**, 489 (2016).

[124]H. Xu, B. Dong, S. Xu, S. Xu, X. Sun, J. Sun, Y. Yang, L. Xu, X. Bai, S. Zhang, Z. Yin, and H. Song, Biomaterials **138**, 69 (2017).
[125]J. Ko, N. Bhagwat, S. S. Yee, T. Black, C. Redlinger, J. Romeo, M. O'Hara, A. Raj, E. L. Carpenter, B. Z. Stanger, and D. Issadore, Lab Chip **17**, 3086 (2017).
[126]W. Shi, S. Wang, A. Maarouf, C. G. Uhl, R. He, D. Yunus, and Y. Liu, Lab Chip **17**, 3291 (2017).
[127]M. Poudineh, P. M. Aldridge, S. Ahmed, B. J. Green, L. Kermanshah, V. Nguyen, C. Tu, R. M. Mohamadi, R. K. Nam, A. Hansen, S. S. Sridhar, A. Finelli, N. E. Fleshner, A. M. Joshua, E. H. Sargent, and S. O. Kelley, Nat. Nanotechnol. **12**, 274 (2017).
[128]H. Chen, Z. Zhang, H. Liu, Z. Zhang, C. Lin, and B. Wang, AIP Adv. **9**, 025023 (2019).
[129]X. Wang, L. Sun, H. Zhang, L. Wei, W. Qu, Z. Zeng, Y. Liu, and Z. Zhu, PeerJ **7**, e6681 (2019).
[130]R. Zhang, B. Le, W. Xu, K. Guo, X. Sun, H. Su, L. Huang, J. Huang, T. Shen, T. Liao, Y. Liang, J. X. J. Zhang, H. Dai, and K. Qian, Small Methods **3**, 1970004 (2019).